

# Using the single quark transition model to predict nucleon resonance amplitudes

G. Ramalho

*International Institute of Physics, Federal University of Rio Grande do Norte,  
Avenida Odilon Gomes de Lima 1722, Capim Macio, Natal-RN 59078-400, Brazil*

(Dated: October 20, 2018)

We present predictions for the  $\gamma^*N \rightarrow N^*$  helicity amplitudes, where  $N^*$  is a member of the  $[70, 1^-]$  supermultiplet. We combine the results from the single quark transition model for the helicity amplitudes with the results of the covariant spectator quark model for the  $\gamma^*N \rightarrow N^*(1535)$  and  $\gamma^*N \rightarrow N^*(1520)$  transitions. The theoretical estimations from the covariant spectator quark model are used to calculate three independent functions  $A, B$ , and  $C$  of  $Q^2$ , where  $Q^2 = -q^2$  and  $q$  is the momentum transfer. With the knowledge of the functions  $A, B$ , and  $C$  we estimate the helicity amplitudes for the transitions  $\gamma^*N \rightarrow N^*(1650)$ ,  $\gamma^*N \rightarrow N^*(1700)$ ,  $\gamma^*N \rightarrow \Delta(1620)$ , and  $\gamma^*N \rightarrow \Delta(1700)$ . The analysis is restricted to reactions with proton targets. The predictions for the transition amplitudes are valid for  $Q^2 > 2 \text{ GeV}^2$ .

## I. INTRODUCTION

One of the challenges of modern physics is the description of the internal structure of the hadrons. It is believed that the substructure of the hadrons in general and the nucleon and the nucleon resonances in particular, are ruled by Quantum Chromodynamics (QCD), in terms of quark and gluon degrees of freedom. Although QCD can be useful for reactions at high  $Q^2$ , it becomes more complex at low and intermediate  $Q^2$ , which restrains the theoretical predictions for that range [1, 2]. Therefore in practice to obtain predictions for small  $Q^2$  one has sometimes to rely on effective degrees of freedom as the constituent quarks.

The quark substructure of a baryon can in first approximation be classified in terms of the  $SU(6)$  spin-flavor symmetry, combined with the  $O(3)$  group for radial and rotational excitations. In that framework the spin 1/2 baryons, including the nucleon, and the spin 3/2 baryons can be classified in supermultiplets  $[SU(6), L^P]$  characterized by angular momentum ( $J$ ), quark total spin ( $S = 1/2, 3/2$ ), orbital angular momentum ( $L$ ) and parity ( $P$ ). In the notation  $[SU(6), L^P]$ ,  $SU(6)$  represents the number of particles of the multiplet (including all spin projections). Then the nucleon ( $J^P = \frac{1}{2}^+$ ) is part of the  $[56, 0^+]$  supermultiplet and the states  $N^*(1535)$  ( $J^P = \frac{1}{2}^-$ ), also represented by  $S_{11}(1535)$ , and  $N^*(1520)$  ( $J^P = \frac{3}{2}^-$ ), also represented by  $D_{13}(1520)$  are part of the  $[70, 1^-]$  supermultiplet [3].

The use of the  $SU(6) \otimes O(3)$  group [3, 4] to represent the wave functions of a baryon (three-quark system) combined with the electromagnetic interaction in impulse approximation leads to the so-called single quark transition model (SQTM) [5–7]. Here, single means that only one quark couples with the photon (impulse approximation). In these conditions the SQTM can be used to parametrize

the transition current between two supermultiplets, in an operational form that includes only four independent terms, with coefficients exclusively dependent of  $Q^2$ .

In particular, the SQTM can be used to parametrize the  $\gamma^*N \rightarrow N^*$  transitions, where  $N^*$  is a nucleon (isospin 1/2) or a  $\Delta$  (isospin 3/2) excitation from the  $[70, 1^-]$  supermultiplet, in terms of three independent functions of  $Q^2$ :  $A, B$ , and  $C$  [1, 5–8]. The relation between the functions  $A, B$ , and  $C$  and the amplitudes are presented in Table I. In the table, besides the transitions  $\gamma^*N \rightarrow S_{11}(1535)$  and  $\gamma^*N \rightarrow D_{13}(1520)$ , one has expressions for the transitions  $\gamma^*N \rightarrow S_{11}(1650)$ ,  $\gamma^*N \rightarrow D_{13}(1700)$ ,  $\gamma^*N \rightarrow S_{31}(1620)$ , and  $\gamma^*N \rightarrow D_{33}(1700)$ . Once the coefficients  $A, B$ , and  $C$  are determined it is possible to predict the transition helicity amplitudes for all the resonances from the  $[70, 1^-]$  supermultiplet. The relations presented in the table are based in the exact  $SU(6)$  spin-flavor symmetry broken by the color-hyperfine interaction between quarks. That interaction leads to the configuration mixing between various baryon states characterized by some mixing angles, estimated from hadron decays [1, 3, 4, 7]. Note however, that as the SQTM is based exclusively on the valence quark degrees of freedom, we should not expect a good description of the reactions at low  $Q^2$ , where meson cloud effects may be very important [1, 2, 8–14]. Calculations for the same helicity amplitudes using quark models can be found in Refs. [1, 8, 9, 15–26].

The covariant spectator quark model was applied in the past to the electromagnetic structure of the nucleon [27] and the  $S_{11}(1535)$ ,  $D_{13}(1520)$  excitations [28, 29]. The determination of the transition helicity amplitudes are based mainly on the valence quark content, but some information about additional effects like the meson cloud dressing can be inferred from the formalism. One can then use the results from the covariant spectator quark model for the  $A_{1/2}$  amplitude in the  $S_{11}(1535)$  transi-

tion and the two transverse amplitudes ( $A_{1/2}$  and  $A_{3/2}$ ) in the  $D_{13}(1520)$  transition, to calculate  $A, B$ , and  $C$ . Note, however, that because the valence quark effects are dominant only at large  $Q^2$ , the results are accurate only in that region. Based on the results of the covariant spectator quark model for the  $\gamma^*N \rightarrow S_{11}(1535)$  and  $\gamma^*N \rightarrow D_{13}(1520)$  transitions we estimate that the predictions of the model should be accurate for the  $Q^2 > 2$  GeV<sup>2</sup> region.

As the covariant spectator quark model breaks the  $SU(2)$ -isospin symmetry, the use of that model to calculate the functions  $A, B$ , and  $C$  from the SQTM has to be understood as an approximation, with a degree of error proportional to the percentage of the  $SU(2)$  breaking. As consequence the estimation for neutral reactions (with neutron targets) will be less reliable, since in the covariant spectator quark model those reactions depend significantly of the  $SU(2)$  breaking. For instance, the neutron electric form factor would vanish if the  $SU(2)$  symmetry breaking was not considered [27].

The article is organized as follows: In the next section we present the relations between the  $\gamma^*N \rightarrow N^*$  amplitudes for the  $N^*$  resonances of the  $[70, 1^-]$  supermultiplet and the functions  $A, B$ , and  $C$ , according to the SQTM. In Sec. III we discuss the formalism of the covariant spectator quark model. The expressions of the covariant spectator quark model for the  $S_{11}(1535)$  and  $D_{13}(1520)$  excitations are presented in Sec. IV. The numerical results for the  $[70, 1^-]$  amplitudes are presented in Sec. V. The summary and the conclusions are in Sec. VI.

## II. DETERMINATION OF THE FUNCTIONS $A, B$ , AND $C$

The expressions for the  $\gamma^*N \rightarrow N^*$  amplitudes for a  $N^*$  resonance from the  $[70, 1^-]$  supermultiplet calculated by the SQTM [7, 8] are presented in Table I. For the mixing angles we use the values from Ref. [7]:  $\theta_S = 31^\circ$  and  $\theta_D = 6^\circ$ . Since the SQTM estimates are derived from the interaction of quarks with transverse photons there are no estimates for the amplitudes  $S_{1/2}$  [7]. Using the table, we can write in particular for the  $S_{11}(1535)$  (label  $S_{11}$ ) and  $D_{13}(1520)$  (label  $D_{13}$ ) cases:

$$A_{1/2}^{S_{11}} = \frac{1}{6}(A + B - C) \cos \theta_S, \quad (2.1)$$

and

$$A_{1/2}^{D_{13}} = \frac{1}{6\sqrt{2}}(A - 2B - C) \quad (2.2)$$

$$A_{3/2}^{D_{13}} = \frac{1}{2\sqrt{6}}(A + C), \quad (2.3)$$

where in the last expressions we approximate  $\cos \theta_D = 0.99 \rightarrow 1$ .

State	Amplitude	
$S_{11}(1535)$	$A_{1/2}$	$\frac{1}{6}(A + B - C) \cos \theta_S$
$D_{13}(1520)$	$A_{1/2}$	$\frac{1}{6\sqrt{2}}(A - 2B - C) \cos \theta_D$
	$A_{3/2}$	$\frac{1}{2\sqrt{6}}(A + C) \cos \theta_D$
$S_{11}(1650)$	$A_{1/2}$	$\frac{1}{6}(A + B - C) \sin \theta_S$
$S_{31}(1620)$	$A_{1/2}$	$\frac{1}{18}(3A - B + C)$
$D_{13}(1700)$	$A_{1/2}$	$\frac{1}{6\sqrt{2}}(A - 2B - C) \sin \theta_D$
	$A_{3/2}$	$\frac{1}{2\sqrt{6}}(A + C) \sin \theta_D$
$D_{33}(1700)$	$A_{1/2}$	$\frac{1}{18\sqrt{2}}(3A + 2B + C)$
	$A_{3/2}$	$\frac{1}{6\sqrt{6}}(3A - C)$

TABLE I: Amplitudes  $A_{1/2}$  and  $A_{3/2}$  estimated by SQTM for the proton targets ( $N = p$ ). The angle  $\theta_S$  is the mixing angle associated with the  $S_{11}$  states ( $\theta_S = 31^\circ$ ). The angle  $\theta_D$  is the mixing angle associated with the  $D_{13}$  states ( $\theta_D = 6^\circ$ ).

From the previous relations, we obtain

$$A = 2 \frac{A_{1/2}^{S_{11}}}{\cos \theta_S} + \sqrt{2} A_{1/2}^{D_{13}} + \sqrt{6} A_{3/2}^{D_{13}} \quad (2.4)$$

$$B = 2 \frac{A_{1/2}^{S_{11}}}{\cos \theta_S} - 2\sqrt{2} A_{1/2}^{D_{13}} \quad (2.5)$$

$$C = -2 \frac{A_{1/2}^{S_{11}}}{\cos \theta_S} - \sqrt{2} A_{1/2}^{D_{13}} + \sqrt{6} A_{3/2}^{D_{13}}. \quad (2.6)$$

An interesting approximation is the case  $A_{3/2}^{D_{13}} \simeq 0$ . From Eq. (2.3) we conclude that the approximation is equivalent to  $A+C \simeq 0$ , or  $C \simeq -A$ , reducing the number of functions to be determined to only 2 ( $A$  and  $B$ ). In the case  $A_{3/2}^{D_{13}} \simeq 0$ , we obtain then

$$A_{1/2}^{S_{11}} \simeq \frac{1}{6}(2A + B) \cos \theta_S, \quad (2.7)$$

$$A_{1/2}^{D_{13}} \simeq \frac{\sqrt{2}}{6}(A - B). \quad (2.8)$$

The study of the  $\gamma^*N \rightarrow D_{13}(1520)$  transition suggests that the amplitude  $A_{3/2}$  falls off faster than  $A_{1/2}$  with  $Q^2$ , justifying the approximation  $A_{3/2} \simeq 0$  for large  $Q^2$  [29]. In the covariant spectator quark model, in particular  $A_{3/2}^{D_{13}} \approx 0$  when the meson cloud effects are not included. Therefore, in that model the results for  $A_{3/2}^{D_{13}}$  are interpreted as the exclusive consequence of the meson cloud effects. However, the falloff of  $A_{3/2}$  is slow when compared with the typical falloff from the meson cloud effects [29]. In order to check if our estimate can be improved in this paper we include also a parametrization for the amplitude  $A_{3/2}^{D_{13}}$ , which simulates the meson cloud effects.

### III. COVARIANT SPECTATOR QUARK MODEL

In the covariant spectator quark model, baryons are treated as three-quark systems. The baryon wave functions are derived from the quark states according to the  $SU(6) \otimes O(3)$  symmetry group. A quark is off-mass-shell, and free to interact with the photon fields, and other two quarks are on-mass-shell [13, 27, 30, 31]. Integrating over the quark-pair degrees of freedom we reduce the baryon to a quark-diquark system, where the diquark can be represented as an on-mass-shell spectator particle with an effective mass of  $m_D$  [27, 29–31].

The electromagnetic interaction with the baryons is described by the photon coupling with the constituent quarks in the relativistic impulse approximation, and the quark electromagnetic structure is represented in terms of the quark form factors parametrized by a vector meson dominance mechanism [27, 31, 32]. The parametrization of the quark current was calibrated in the studies of the nucleon form factors [27], by the lattice QCD data for the decuplet baryons [31], and encodes effectively the gluon and quark-antiquark substructure of the constituent quarks.

The quark current has the general form [27, 31]

$$j_q^\mu(Q^2) = j_1(Q^2)\gamma^\mu + j_2(Q^2)\frac{i\sigma^{\mu\nu}q_\nu}{2M}, \quad (3.1)$$

where  $M$  is the nucleon mass and  $j_i$  ( $i = 1, 2$ ) are the Dirac and Pauli quark form factors. In the  $SU(2)$ -flavor sector the functions  $j_i$  can also be decomposed into the isoscalar ( $f_{i+}$ ) and the isovector ( $f_{i-}$ ) components

$$j_i(Q^2) = \frac{1}{6}f_{i+}(Q^2) + \frac{1}{2}f_{i-}(Q^2)\tau_3, \quad (3.2)$$

where  $\tau_3$  acts on the isospin states of baryons (nucleon or resonance). The details can be found in Refs. [13, 27, 31]. Since the quark current includes a Pauli term, the quarks have nonzero anomalous magnetic moment ( $\kappa_q$ ) in the present formalism.

In the study of inelastic reactions (the final state has a mass different from the initial state) we replace  $\gamma^\mu \rightarrow \gamma^\mu - \frac{q^\mu}{q^2}$  in Eq. (3.1). This procedure is equivalent to the use of the Landau prescription in the transition current and ensures the conservation of the transition current between the baryon states [33–35]. The term restores current conservation but does not affect the results of the observables [33].

When the nucleon ( $\Psi_N$ ) and the final resonance  $R$  ( $\Psi_R$ ), where  $R$  stands for a  $N^*$  nucleon resonance, wave functions are written in terms of the single quark and quark-pair states, the transition current can be written in the relativistic impulse approximation [27, 30, 31] as

$$J^\mu = 3 \sum_{\Gamma} \int_k \bar{\Psi}_R(P_+, k) j_q^\mu \Psi_N(P_-, k), \quad (3.3)$$

where  $P_-$ ,  $P_+$ , and  $k$  are the nucleon, the resonance, and the diquark momenta respectively. In the previous equation the index  $\Gamma$  labels the possible states of the intermediate diquark, the factor 3 takes account of the contributions from the other quark pairs by the symmetry, and the integration symbol represents the covariant integration over the diquark on-mass-shell momentum.

In the calculation of the transition current it is convenient to project the states on the isospin symmetric components (label  $S$ ) or the isospin antisymmetric components (label  $A$ ). We can define then, the  $Q^2$  dependent coefficients

$$j_i^A = \frac{1}{6}f_{i+} + \frac{1}{2}f_{i-}\tau_3 \quad (3.4)$$

$$j_i^S = \frac{1}{6}f_{i+} - \frac{1}{6}f_{i-}\tau_3. \quad (3.5)$$

See Refs. [13, 27, 31] for more details. For future discussion we note that

$$j_i^A + \frac{1}{3}j_i^S = \frac{2}{9}(f_{i+} + 2f_{i-}\tau_3). \quad (3.6)$$

Using Eq. (3.3), we can express the transition current in terms of the coefficients  $j_i^{A,S}$  and the radial wave functions  $\psi_N$  and  $\psi_R$  [27–29]. The radial wave functions are scalar functions that depend on the baryon and diquark momenta. Those functions parametrize the momentum distributions of the quark-diquark systems. From the transition current we can extract the form factors and the helicity transition amplitudes, defined in the rest frame of the resonance (final state), for the reaction under study [1, 2, 28, 29].

As mentioned, the representation of the quark current in terms of a vector meson dominance parametrization [13, 27, 31] simulates in an effective way the internal structure of the constituent quarks, including the meson cloud dressing of the quarks. There are however some processes such as the meson exchanged between the different quarks inside the baryon, which cannot be reduced to simple diagrams with quark dressing. Those processes are regarded as arising from a meson exchanged between the different quarks inside the baryon and can be classified as meson cloud corrections to the hadronic reactions [13, 14, 29].

The covariant spectator quark model was already applied to the  $\Delta(1232)$  system [36, 37], to some nucleon resonances like the Roper,  $N^*(1520)$ ,  $N^*(1535)$ ,  $N^*(1710)$  and  $\Delta(1600)$  [28, 29, 38, 39] and several reactions with strange baryons [14, 40, 41].

In the present work the necessary input from the covariant spectator quark model is the transition form factors (that can be rewritten as helicity amplitudes) for the  $\gamma^*N \rightarrow N^*$  transitions with  $N^* = S_{11}(1535), D_{13}(1520)$ . The  $\gamma^*N \rightarrow S_{11}(1535)$  and  $\gamma^*N \rightarrow D_{13}(1520)$  transitions were analyzed in Refs. [28, 29]. In those papers we used the parametrization of the nucleon system given by Ref. [27], which requires two parameters to describe the radial wave function  $\psi_N$ , and the parametrization of

the quark current described below. In order to obtain a complete representation of the systems  $S_{11}(1535)$  and  $D_{13}(1520)$ , one has to define convenient radial wave functions that ensures the orthogonality between those wave functions with the nucleon wave function. The subject is discussed in the Appendix. for the  $S_{11}(1535)$  case, and in Ref. [29] for the  $D_{13}(1520)$  case. In simple words we can say that we define the  $N^*$  radial wave functions with the same long range parametrization as the nucleon and define a new short range parameter for each resonance. Therefore, we add to the model of the nucleon one new parameter for resonance. For the case of the  $D_{13}(1520)$ , we include a simple parametrization of the meson cloud, as discussed in Ref. [29], in order to reproduce the amplitude  $A_{3/2}$ .

#### IV. PARAMETRIZATION OF $S_{11}(1535)$ AND $D_{13}(1520)$ AMPLITUDES

We will discuss now the parametrizations of the amplitudes associated with the  $\gamma^*N \rightarrow S_{11}(1535)$  and  $\gamma^*N \rightarrow D_{13}(1520)$  transitions. To distinguish between the two cases we will use the label  $S$  (or  $S_{11}$ ) for the  $S_{11}$  state, and the label  $D$  (or  $D_{13}$ ) for the  $D_{13}$  state. Then  $M_S$  represents the  $S_{11}$  mass ( $\approx 1.535$  GeV) and  $M_D$  represents the  $D_{13}$  mass ( $\approx 1.520$  GeV). The details of the structure of those systems can be found in Refs. [28, 29]. Here we will discuss only the main features of those transitions.

For the  $\gamma^*N \rightarrow S_{11}(1535)$  we consider the calculation from Ref. [28], developed for the high  $Q^2$  region, that we extend in the present work also to the low  $Q^2$  region. The details are presented in the Appendix. Recall that the  $S_{11}(1535)$  state is described in the present model using exclusively the valence quark degrees of freedom. The interesting properties of the  $S_{11}(1535)$  amplitudes are also discussed in Refs. [41, 42].

For the  $\gamma^*N \rightarrow D_{13}(1520)$  transition we use the model from Ref. [29], particularly for the valence quark contributions. Since one of the amplitudes ( $A_{3/2}$ ) vanishes in the covariant spectator quark model formalism, when only the valence quark contributions are taken into account, we investigate also the impact of considering a meson cloud parametrization for that amplitude.

##### A. Resonance $S_{11}(1535)$

The electromagnetic structure of the  $\gamma^*N \rightarrow S_{11}(1535)$  transition can be parametrized by two independent form factors  $F_1^*$  and  $F_2^*$  [28, 42]. The experimental data suggests that  $F_2^* \simeq 0$  for large  $Q^2$ , more specifically for  $Q^2 > 1.5$  GeV<sup>2</sup>. As for the  $F_1^*$ , the data are well described by the covariant spectator quark model. Combining both results, for large  $Q^2$  we can calculate  $A_{1/2}$

using

$$A_{1/2} = -\frac{\sqrt{2}}{3}F_S(f_{1+} + 2f_{1-\tau_3})\mathcal{I}_{S_{11}}\cos\theta_S, \quad (4.1)$$

where

$$\mathcal{I}_{S_{11}}(Q^2) = \int_k \frac{k_z}{|\mathbf{k}|} \psi_{S_{11}}(P_+, k) \psi_N(P_-, k), \quad (4.2)$$

and

$$F_S = 2e\sqrt{\frac{(M_S + M)^2 + Q^2}{8M(M_S^2 - M^2)}}. \quad (4.3)$$

In the previous equations  $\mathcal{I}_{S_{11}}$  gives an integral defined in the  $S_{11}$  rest frame, but it can also be written in a covariant form [28]. In the  $S_{11}$  rest frame one has  $P_+ = (M_S, 0, 0, 0)$  and  $P_- = (\sqrt{M^2 + |\mathbf{q}|^2}, 0, 0, -|\mathbf{q}|)$ , where  $|\mathbf{q}|$  is the magnitude of the photon three-momentum.

As mentioned already, the experimental result for  $F_2^*$  vanishes for  $Q^2 > 1.5$  GeV<sup>2</sup> [28]. This can be interpreted as a consequence of the cancellation between valence quark and meson cloud effects [28, 41, 42]. Therefore, although the estimate from the valence quark contribution is nonzero, if we want to estimate the final result for  $F_2^*$ , the best approximation is  $F_2^* = 0$ . A consequence of the previous result is that we obtain the best estimate for  $A_{1/2}$  when we neglect  $F_2^*$  in the calculations.

At the moment we discuss the  $S_{11}(1535)$  state under the assumption that the contributions with core spin 1/2 (core spin is the sum of the quark spins), are the more important components of the wave function (contributions proportional to  $\cos\theta_S$ ). However, the  $S_{11}(1535)$  state has also contributions from states with core spin 3/2 (proportional to  $\sin\theta_S$ ). Those contributions were not calculated at the moment in the context of the covariant spectator quark model framework, although that can be done in the future, using the formalism developed in Ref. [29].

As we did not include the possible effects of the core spin 3/2 component, it may happen that we are underestimating the magnitude of the amplitude  $A_{1/2}$ . However, the explicit inclusion of those effects would also reduce the previous result from the spin 1/2 component from Ref. [28], since we need to correct that value by  $\cos\theta_S$ , because the limit  $\cos\theta_S = 1$  was used in that work. To accommodate the core spin 3/2 components in an effective way we simply take Eq. (4.1) with  $\cos\theta_S = 1$ . Future calculations can test the previous assumption. However, for the propose of the present work we did not expect that the results would be significantly affected by the explicit inclusion of the terms with  $\sin\theta_S$ , which are omitted in the present calculation.

## B. Resonance $D_{13}(1520)$

The valence quark contributions for the  $\gamma^*N \rightarrow D_{13}(1520)$  form factors can be written as [29]

$$G_M = \frac{1}{3\sqrt{3}} \frac{M}{M_D - M} \sqrt{\frac{(M_D - M)^2 + Q^2}{(M_D + M)^2 + Q^2}} \times \left[ (f_{1+} + 2f_{1-\tau_3}) + \frac{M_D + M}{2M} (f_{2+} + 2f_{2-\tau_3}) \right] \mathcal{I}_{D_{13}}, \quad (4.4)$$

$$G_E = -G_M, \quad (4.5)$$

where

$$\mathcal{I}_{D_{13}}(Q^2) = \int_k \frac{k_z}{|\mathbf{k}|} \psi_{D_{13}}(P_+, k) \psi_N(P_-, k). \quad (4.6)$$

The expression for the Coulomb quadrupole form factor  $G_C$  is not relevant for the present work, since the SQTm expressions do not apply to the  $S_{1/2}$  amplitude. Also, in the last case the integral is represented in the resonance  $D_{13}$  rest frame:  $P_+ = (M_D, 0, 0, 0)$  and  $P_- = (\sqrt{M^2 + |\mathbf{q}|^2}, 0, 0, -|\mathbf{q}|)$ , where  $|\mathbf{q}|$  is the magnitude of the photon three-momentum.

From the form factors, we can calculate the helicity amplitudes, using [29]

$$A_{1/2} = F_D G_M + \frac{1}{4} F_D G_4^\pi \quad (4.7)$$

$$A_{3/2} = \frac{\sqrt{3}}{4} F_D G_4^\pi \quad (4.8)$$

where

$$F_D = \frac{e}{M} \sqrt{\frac{M_D - M}{M_D + M}} \sqrt{\frac{(M_D + M)^2 + Q^2}{2M}}. \quad (4.9)$$

In the Eqs. (4.7)-(4.8),  $G_4^\pi$  is a new function, which vanishes if only the valence quark contributions are considered, but that can be used to parametrize the pion and other meson cloud effects.

The fit to the  $A_{3/2}$  data gives

$$G_4^\pi = 1.354 \left( \frac{\Lambda_4^2}{\Lambda_4^2 + Q^2} \right)^3 F_\rho, \quad (4.10)$$

where  $\Lambda_4^2 = 20 \text{ GeV}^2$ . The function  $F_\rho$  is defined as

$$F_\rho = \frac{m_\rho^2}{m_\rho^2 + Q^2 + \frac{1}{\pi} \frac{\Gamma_\rho^0}{m_\pi} Q^2 \log \frac{Q^2}{m_\pi^2}}. \quad (4.11)$$

In the last expression,  $m_\rho$  and  $m_\pi$  are the  $\rho$  and pion mass, respectively and  $\Gamma_\rho^0 = 0.149 \text{ GeV}$  [29].

Note that the parametrization of the amplitude  $A_{3/2}$  given by Eqs. (4.8) and (4.10) is in the region  $Q^2 = 5\text{--}10 \text{ GeV}^2$ , dominated by the function  $F_\rho \propto 1/(Q^2 \log Q^2)$  due to the large cutoff ( $\Lambda_4^2 = 20 \text{ GeV}^2$ ) in the tripole

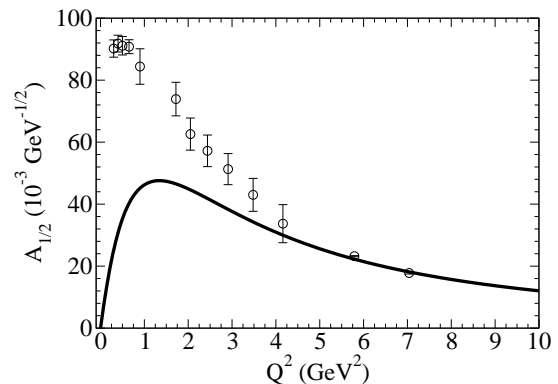


FIG. 1: Results for the  $\gamma^*p \rightarrow S_{11}^+(1535)$  amplitude  $A_{1/2}$ . Data-points from CLAS [44] and JLab/Hall C [45].

factor. Therefore in the intermediate  $Q^2$  region,  $A_{3/2}$  shows a slow falloff, contrary to what we would expect from a meson cloud contribution.

It is worth mentioning that other quark models predict nonzero contributions for the amplitude  $A_{3/2}$  [15–20, 22–25]. However, those estimates are small in general, and about 20-40% of the measured values [15, 18–20, 22–25]. Those results can be interpreted as an indication that the meson cloud effects are the dominant contribution for the amplitude  $A_{3/2}$ , as assumed in Ref. [29] in the context of the covariant spectator quark model. Also the results of the Excited Baryon Analysis Center (EBAC) coupled-channel reaction model supports the idea that the meson cloud effects are the dominant contribution for the amplitude  $A_{3/2}$  [43].

## V. RESULTS

We will present the results in the following way: First we show the results from the covariant spectator quark model for the  $\gamma^*N \rightarrow S_{11}(1535)$  and  $\gamma^*N \rightarrow D_{13}(1520)$  amplitudes. Next we calculate the functions  $A$ ,  $B$ , and  $C$  using the expressions derived in Sec. II. Finally we use the functions  $A$ ,  $B$ , and  $C$  to estimate the amplitudes  $A_{1/2}$  and  $A_{3/2}$  for the remaining electromagnetic transitions.

### A. Model for the $\gamma^*N \rightarrow S_{11}(1535)$ and $\gamma^*N \rightarrow D_{13}(1520)$ amplitudes

The results of amplitude  $A_{1/2}$  for the  $\gamma^*N \rightarrow S_{11}(1535)$  transition, given by Eq. (4.1), are presented in Fig. 1. The deviation between model and data at low  $Q^2$  can be the consequence of the meson cloud not included in the model. For the  $S_{1/2}$  there are evidences that it is correlated with  $A_{1/2}$  at large  $Q^2$  [42].

The results of the amplitudes  $A_{1/2}$  and  $A_{3/2}$  relative for transition  $\gamma^*N \rightarrow D_{13}(1520)$  are presented in Fig. 2. For the amplitude  $A_{1/2}$ , given by Eq. (4.7) we consider

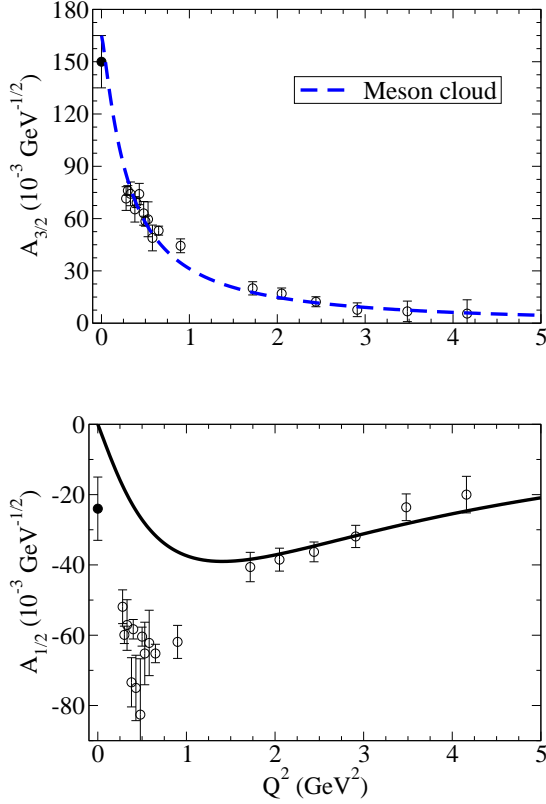


FIG. 2: Results for the  $\gamma^*p \rightarrow D_{13}^+(1520)$  amplitudes  $A_{1/2}$  and  $A_{3/2}$ . Data from CLAS [44, 46] and PDG [47].

only the valence quark contributions given by Eq. (4.4) and drop the term  $G_4^\pi$ . As for  $A_{3/2}$ , since the valence quark contributions vanishes (in the limit  $\sin\theta_D \rightarrow 0$ ), we present the result obtained by the parametrization of the meson cloud given by Eq. (4.8).

From Figs. 1 and 2 we may conclude that one has a good description of the data (about two standard deviations) for the  $\gamma^*N \rightarrow N^*(1535)$  transition when  $Q^2 > 2.5$   $\text{GeV}^2$  and for the  $\gamma^*N \rightarrow N^*(1520)$  transition when  $Q^2 > 1.5$   $\text{GeV}^2$ . We may then say that the covariant spectator quark model is reliable for  $Q^2 > 2$   $\text{GeV}^2$ .

### B. Calculation of $A, B,$ and $C$

In the calculation of the coefficients  $A, B,$  and  $C$  we consider two different approximations:

- **Model 1:** we use the approximation  $A_{3/2}^{D13} \equiv 0$ , based on Eqs. (2.7)-(2.8), and calculate the two independent functions ( $A$  and  $B$ ). The results are represented by a dashed line. In this case only valence quark degrees of freedom are considered.
- **Model 2:** we include the parametrization of the meson cloud effects for the amplitude  $A_{3/2}^{D13}$  given by Eq. (4.10), and calculate the three coefficients

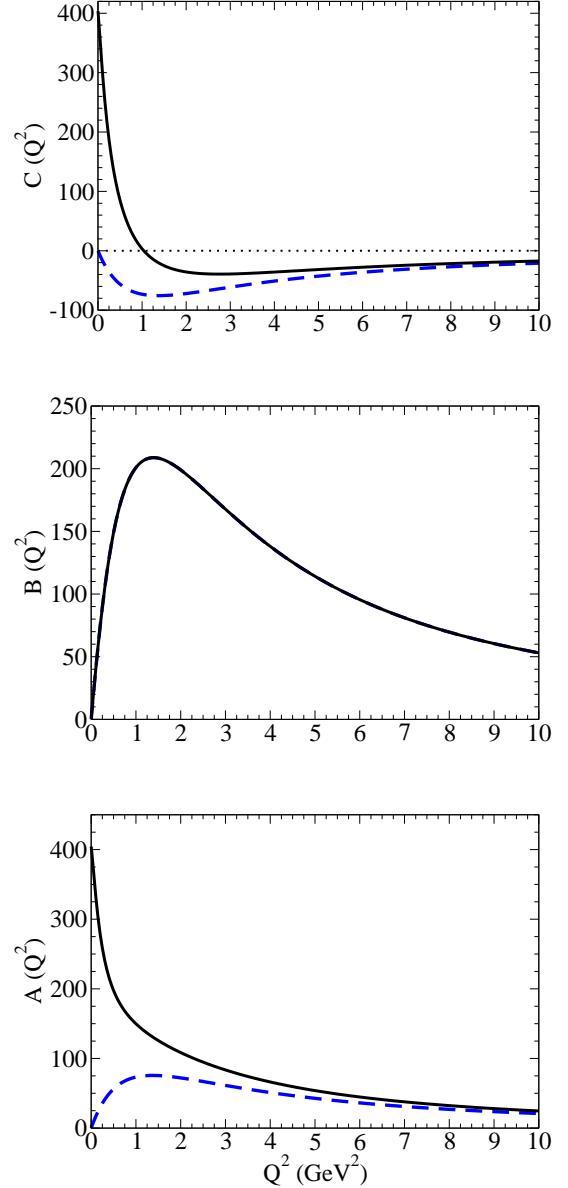


FIG. 3: Coefficients  $A, B,$  and  $C$  for the model 1 (dashed line), model 2 (solid line), according to Eqs. (2.4)-(2.6). For model 1,  $C = -A$ .  $B$  is the same in both models.

using Eqs. (2.4)-(2.6). The results are represented by a solid line.

The results for coefficients  $A, B,$  and  $C$  are presented in Fig. 3 for model 1 (dashed line) and model 2 (solid line).

Note that the function  $B$  is the same for both models, since it is independent of  $A_{3/2}^{D13}$  [see Eq. (2.5)]. For future discussion we note also that the difference  $A - C$  is also the same in both models [see Eqs. (2.4) and (2.6)]. From Table I we may then conclude that the amplitudes  $A_{1/2}$  will be the same for both models for the cases  $S_{11}(1650)$  and  $D_{13}(1700)$ .

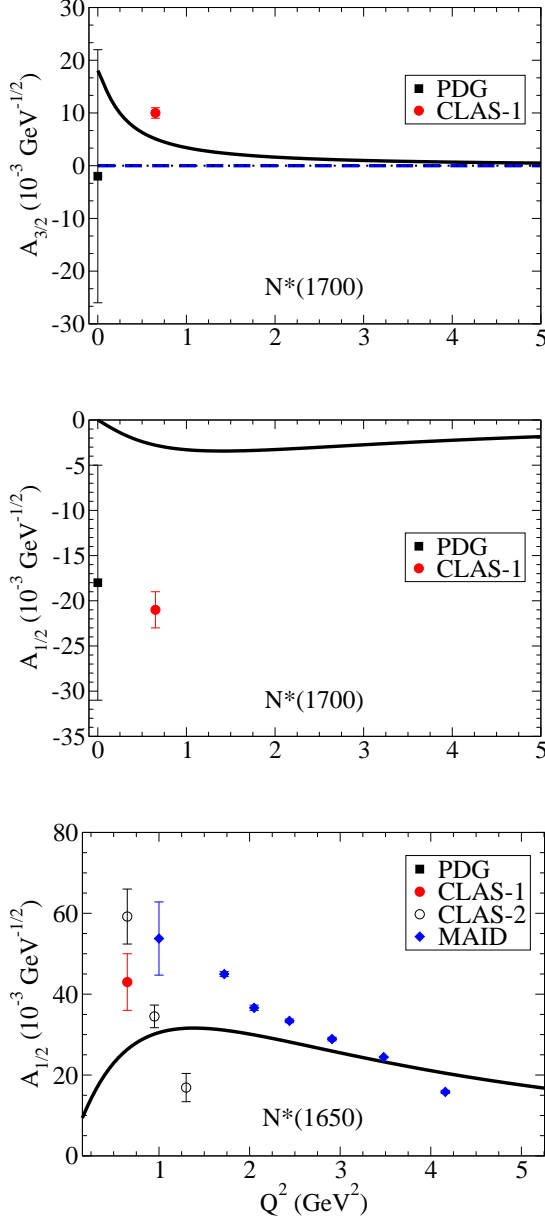


FIG. 4: Amplitudes for the  $\gamma^*p \rightarrow S_{11}^+(1650)$  and  $\gamma^*p \rightarrow D_{13}^+(1700)$  transitions. Model 1 (dashed line) and model 2 (solid line). CLAS data from Refs. [48, 49], MAID data from Refs. [51, 52] and PDG data from Ref. [47].

### C. $\gamma^*N \rightarrow N^*$ amplitudes

Using the parametrization from the SQTm of the amplitudes  $A_{1/2}$  and  $A_{3/2}$  given in Table I, and the results of the coefficients  $A$ ,  $B$ , and  $C$  presented in Fig. 3, we can calculate the amplitudes for the transitions  $\gamma^*N \rightarrow N^*(1650)$ ,  $\gamma^*N \rightarrow N^*(1700)$ ,  $\gamma^*N \rightarrow \Delta(1620)$ , and  $\gamma^*N \rightarrow \Delta(1700)$ , relative to the reactions with proton targets. We recall that the range of application of the model is  $Q^2 > 2 \text{ GeV}^2$ .

We compare our results with the CLAS data from

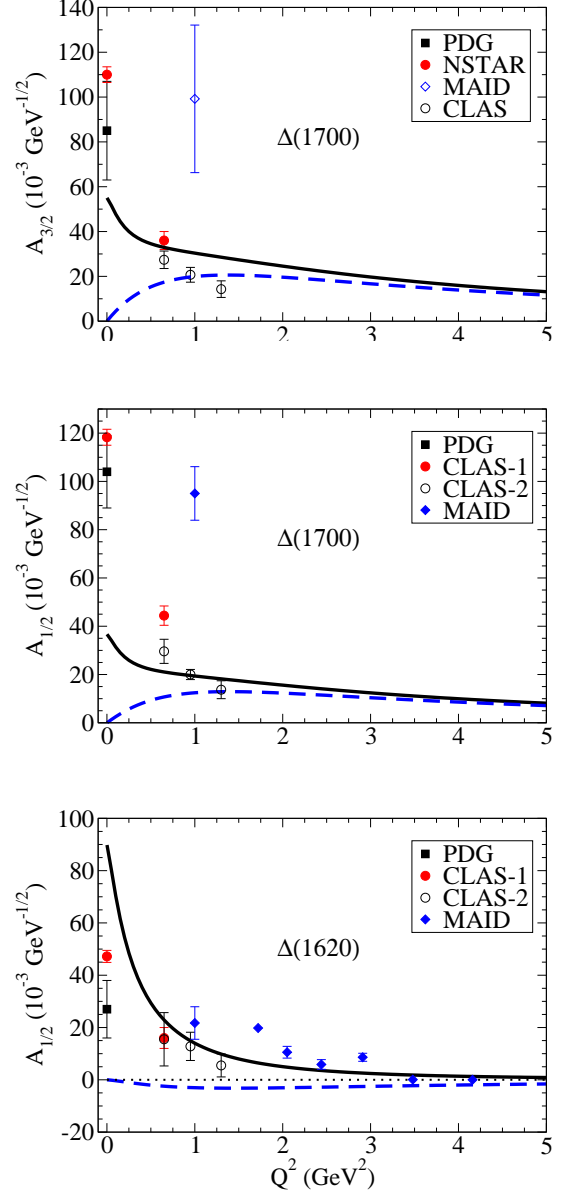


FIG. 5: Amplitudes for the  $\gamma^*p \rightarrow S_{31}^+(1620)$  and  $\gamma^*p \rightarrow D_{33}^+(1700)$  transitions. Model 1 (dashed line) and model 2 (solid line). CLAS data from Refs. [48, 49], MAID data from Refs. [51, 52] and PDG data from Ref. [47].

Refs. [48, 49], labeled as CLAS-1; preliminary data from CLAS, labeled as CLAS-2 [2, 50]; MAID data [51, 52], and PDG data for  $Q^2 = 0$  [47]. The CLAS-1 data include data at the photon point [49] (single pion production) and at  $Q^2 = 0.65 \text{ GeV}^2$  (double pion production) [48]. Not included are the data from Refs. [7, 53] composed by single pion production only and results presented in proceedings, conferences, and workshops.

The estimates based on the SQTm formalism for the helicity amplitudes relative to the  $\gamma^*N \rightarrow S_{11}(1650)$  and  $\gamma^*N \rightarrow D_{13}(1700)$  transitions are presented in Fig. 4. In the figure, models 1 and 2 for the amplitudes  $A_{1/2}$

are indistinguishable because  $A - C$  is the same for both models, as discussed previously. The amplitude  $A_{3/2}$  for the  $\gamma^*N \rightarrow D_{13}(1700)$  transition, vanishes in model 1, because  $A + C = 0$  in that case (by construction). We may conclude then that model 1 is insufficient to describe the data. For that reason and also because of the results for the  $\gamma^*N \rightarrow D_{13}(1520)$  transition in the following we favor model 2.

From the graph for the  $\gamma^*N \rightarrow S_{11}(1650)$  transition we conclude that both models have the same magnitude as the data, although the MAID data have very small errorbars. As for the  $\gamma^*N \rightarrow D_{13}(1700)$  transition, one cannot draw too many conclusions, since there are no data available for large  $Q^2$ , except that our estimate for model 2 is close to the datapoint from CLAS-1 for  $A_{3/2}$ , and it is possible that model 2 can provide a good estimate for larger  $Q^2$ . For the amplitude  $A_{1/2}$  the model underestimate in absolute value the data at low  $Q^2$ .

The results for the  $\gamma^*N \rightarrow S_{31}(1620)$  and  $\gamma^*N \rightarrow D_{33}(1700)$  transitions are presented in Fig. 5. For the  $\gamma^*N \rightarrow S_{31}(1620)$  we conclude that the model 1 gives the wrong sign and magnitude for the  $A_{1/2}$  amplitude. As for the  $\gamma^*N \rightarrow D_{33}(1700)$ , model 1 approaches the results from model 2 when  $Q^2$  increases. Back to the  $\gamma^*N \rightarrow S_{31}(1620)$  transition we conclude that model 2 is close to the data for  $Q^2 > 1 \text{ GeV}^2$  and underestimates the MAID data by about 1-2 standard deviations, since the errorbars are very small. For the  $\gamma^*N \rightarrow D_{33}(1700)$  transition, we cannot conclude much, because there are no data for  $Q^2 > 1.5 \text{ GeV}^2$ , except that both models are close to the CLAS-2 data for  $Q^2 > 1 \text{ GeV}^2$ , and therefore they may be used to make projections for high  $Q^2$ .

In order to check the predictions shown in Figs. 4 and 5, new data on the resonances with masses above 1.6 GeV are needed for  $Q^2 > 2 \text{ GeV}^2$ , where the estimate for quark core contributions can be confronted to the data. The data on double charged pion electroproduction for  $Q^2 = 2\text{--}5 \text{ GeV}^2$  expected from the experiments with the CLAS detector, will allow us for the first time to explore most of the resonances in a mass range up to 2.0 GeV for  $Q^2 < 5 \text{ GeV}^2$  [55].

#### D. Parametrization for high $Q^2$

In order to facilitate the comparison with future experimental data, we derived simple analytic approximations for our numerical results at large  $Q^2$ . Based in the expected large  $Q^2$  behavior:  $A_{1/2} \propto 1/Q^3$  and  $A_{3/2} \propto 1/Q^5$  [54], we choose for large  $Q^2$ , the forms

$$A_{1/2}(Q^2) = D \left( \frac{\Lambda^2}{\Lambda^2 + Q^2} \right)^{3/2} \quad (5.1)$$

$$A_{3/2}(Q^2) = D \left( \frac{\Lambda^2}{\Lambda^2 + Q^2} \right)^{5/2}. \quad (5.2)$$

In the previous expressions  $D$  is a coefficient and  $\Lambda$  a cutoff that depend on the amplitude ( $A_{1/2}$  or  $A_{3/2}$ ) and

State	Amplitude	$D(10^{-3} \text{ GeV}^{-1/2})$	$\Lambda^2 (\text{GeV}^2)$
$S_{11}(1650)$	$A_{1/2}$	68.90	3.35
$S_{31}(1620)$	$A_{1/2}$	...	...
$D_{13}(1700)$	$A_{1/2}$	-8.51	2.82
	$A_{3/2}$	4.36	3.61
$D_{33}(1700)$	$A_{1/2}$	39.22	2.69
	$A_{3/2}$	42.15	8.42

TABLE II: Parameters from the high  $Q^2$  parametrization, according to Eqs. (5.1)-(5.2).

transition. We note however that these parametrizations are valid for a restricted region of  $Q^2$ , since in the covariant spectator quark model the form factors and amplitudes are affected by logarithm corrections in  $Q^2$  for large  $Q^2$  [28, 29, 36].

All amplitudes, except for the  $\gamma^*N \rightarrow S_{31}(1620)$  transition, are well described by the analytic forms of Eqs. (5.1)-(5.2). The numerical results for  $D$  and  $\Lambda^2$  are presented in Table II. The parameters were calculated in order to reproduce the results from model 2 exactly for  $Q^2 = 5 \text{ GeV}^2$ , but they also provide good approximations for values of  $Q^2$  up to  $10 \text{ GeV}^2$ , or even larger.

We found out that the amplitude  $A_{1/2}$  for the transition  $\gamma^*N \rightarrow S_{31}(1620)$  cannot be approximated by Eq. (5.1), in particular by the power 3/2. The falloff of that amplitude is consistent with a stronger falloff. In order to interpret that result we start noting that we can write, using Table I and Eqs. (2.4)-(2.6),

$$A_{1/2}^{S_{31}} \propto \left( 2 \frac{A_{1/2}^{S_{11}}}{\cos \theta_S} + 4\sqrt{2}A_{1/2}^{D_{13}} + 4\sqrt{6}A_{3/2}^{D_{13}} \right). \quad (5.3)$$

If the amplitudes  $A_{1/2}^{S_{11}}, A_{1/2}^{D_{13}} \propto 1/Q^3$ , as expected, the deviation from  $A_{1/2}^{S_{31}}$  from  $1/Q^3$  is a consequence of a partial cancellation between the two amplitudes  $A_{1/2}$  in Eq. (5.3). This interpretation makes sense because those amplitudes have different signs (see Figs. 1 and 2). Due to the cancellation between the leading order term  $\mathcal{O}(1/Q^3)$  of the first two terms,  $A_{1/2}^{S_{31}}$  is dominated by the second order terms and the amplitude  $A_{3/2}^{D_{13}}$ . A simple empirical parametrization of the amplitude in units of  $10^{-3} \text{ GeV}^{-1/2}$  is  $A_{1/2}^{S_{31}} = 77.21 \left( \frac{\Lambda^2}{\Lambda^2 + Q^2} \right)^{5/2}$ , with  $\Lambda^2 = 1 \text{ GeV}^2$ .

## VI. SUMMARY AND CONCLUSIONS

In this work we combined the features of the covariant spectator quark model and the single quark transition model to predict the transition amplitudes  $A_{1/2}, A_{3/2}$  for the transitions  $\gamma^*N \rightarrow S_{11}(1650), \gamma^*N \rightarrow D_{13}(1700)$ ,

$\gamma^*N \rightarrow S_{31}(1620)$ , and  $\gamma^*N \rightarrow D_{33}(1700)$ . The resonances in the final state are all members of the  $[70, 1^-]$  supermultiplet. We follow the method used in Refs. [1, 7, 8], but we use a theoretical model (quark model) to extract the characteristic coefficients associated with the transition, instead of the experimental data, which are contaminated by meson cloud effects at small  $Q^2$ .

Since the covariant spectator quark model and the SQTm are based in the valence quark degrees of freedom, the range of application of the models is the region of intermediate and high  $Q^2$ . In the present case we may define that region as  $Q^2 > 2 \text{ GeV}^2$ , based on the results for the transitions used in the calibration of the SQTm model. The region  $Q^2 > 2 \text{ GeV}^2$  is where meson cloud effects are expected to play a minor role. However, since the covariant spectator quark model predicts that  $A_{3/2} = 0$  for the  $\gamma^*N \rightarrow D_{13}(1520)$  transition, we explore the possibility of improving our estimations including a meson cloud parametrization of that amplitude. We recall that the proposed parametrization for the meson cloud contribution has a very slow falloff (large cutoff  $\Lambda_4^2$ ), which is more typical of a valence quark contribution than from a meson cloud effect contribution. The inclusion of a parametrization of the amplitude  $A_{3/2}$  allows a much better description of the data for intermediate  $Q^2$ , although for much larger  $Q^2$  ( $Q^2 > 5 \text{ GeV}^2$ ), the models with  $A_{3/2} = 0$  and  $A_{3/2} \neq 0$  are very similar.

To facilitate the comparison with future experimental data at high  $Q^2$ , we present also simple parametrizations of the amplitudes  $A_{1/2}$  and  $A_{3/2}$  for the different transitions, compatible with the expected falloff at high  $Q^2$ :  $A_{1/2} \propto 1/Q^3$ ,  $A_{3/2} \propto 1/Q^5$ . The exception to the previous rules is the amplitude  $A_{1/2}$  for the  $\gamma^*N \rightarrow S_{31}(1620)$  transition, where we predict a falloff faster than  $1/Q^3$ .

Summarizing, we present predictions for the  $[70, 1^-]$  amplitudes in the region  $Q^2 > 2 \text{ GeV}^2$ , where we can expect a dominance of the valence quark degrees of freedom. Nevertheless the meson cloud contributions may still be important for some electromagnetic transitions. In addition we present parametrizations for the region  $Q^2 \approx 5 \text{ GeV}^2$ , or larger, that can be tested in the future JLab-12 GeV upgrade.

### Acknowledgments

The author wants to thank Viktor Mokeev and Ralf Gothe for reading the manuscript and for the helpful discussions, comments and suggestions. The author thanks also Viktor Mokeev for sharing the preliminary data from CLAS, labeled here as CLAS-2. This work was supported by the Brazilian Ministry of Science, Technology and Innovation (MCTI-Brazil).

### Appendix A: New parametrization for the $S_{11}(1535)$ amplitudes

The  $S_{11}$  system and the  $\gamma^*N \rightarrow S_{11}(1535)$  transition were studied in Ref. [28] within the covariant spectator quark model formalism. In that paper it was assumed that the diquark was pointlike. If we use a more detailed treatment, where nonpointlike diquark states are considered, following the formalism of Ref. [29], one has to correct the normalization factor from  $N = \frac{1}{2}$  to  $N = \frac{1}{\sqrt{2}}$ , reducing the first estimate by a factor  $1/\sqrt{2}$ . The final expression for the Dirac form factor  $F_1^*$  is then

$$F_1^* = \frac{\sqrt{2}}{3} (f_{1+} + 2f_{1-}\tau_3) \mathcal{I}_{S_{11}}. \quad (\text{A1})$$

Another aspect that can be improved in the model from Ref. [28] is the low  $Q^2$  region dependence of the form factors. In the model from Ref. [28], the nucleon and the  $S_{11}$  states were not strictly orthogonal therefore the model failed near  $Q^2 = 0$ , because  $\mathcal{I}_{S_{11}}(0) \neq 0$  and  $A_{1/2}(0) \rightarrow \infty$ . The exact orthogonality between those states demands  $\mathcal{I}_{S_{11}}(0) = 0$ . We can fix that problem redefining the radial wave function in order to obtain  $\mathcal{I}_{S_{11}}(0) = 0$ . The price to pay is the introduction of a new parameter in the radial wave function  $\psi_{S_{11}}$ , which can be fixed by a fit to the data, as explained next. The same procedure was used in Ref. [29] for the  $D_{13}(1520)$  wave function.

We note however that even in the present case, where the model is valid near  $Q^2 = 0$ , we cannot expect a very good agreement between model and experimental data at low  $Q^2$ , because the meson cloud effects are not included.

#### 1. Imposing the orthogonality between states

In general, in the covariant spectator quark model the radial wave functions can be expressed in terms of the variable  $(P - k)^2$ , where  $P$  and  $k$  are respectively the baryon and the diquark momenta, because the baryon and the diquark are both on-mass-shell. The dependence in the momenta can then be represented using the dimensionless variable

$$\chi = \frac{(M_B - m_D)^2 - (P - k)^2}{M_B m_D}, \quad (\text{A2})$$

where  $M_B$  and  $m_D$  are respectively the baryon and diquark masses.

In that case the nucleon wave function is defined as

$$\psi_N(P, k) = \frac{N_0}{m_D(\beta_1 + \chi)(\beta_2 + \chi)}, \quad (\text{A3})$$

where  $N_0$  is a normalization constant and  $\beta_1, \beta_2$  are parameters determined in Ref. [27] by a fit to the nucleon form factor data (model II). The numerical values are  $\beta_1 = 0.049$  and  $\beta_2 = 0.717$ . As  $\beta_2 > \beta_1$ ,  $\beta_1$  parametrizes

the long range region and  $\beta_2$  the short range region, in the coordinate space.

The overlap integral (4.2) includes also the  $S_{11}$  radial wave function. In Ref. [28] we define  $\psi_{S_{11}}$  by the same expression given for the nucleon by Eq. (A3), except for the momentum and mass of the baryon. The problem of that choice is that the integral  $\mathcal{I}_{S_{11}}(0)$  does not vanish, except in the case  $M_S = M$  (nucleon and  $S_{11}$  with the same mass). The reason why  $\mathcal{I}_{S_{11}}(0) \neq 0$ , unless  $M_S = M$ , is because  $S_{11}$  and the nucleon cannot be at rest in the same frame. See Ref. [28] for a complete discussion.

We can avoid that problem, defining  $\psi_{S_{11}}$  in order to be orthogonal to the nucleon. We consider then the form

$$\psi_{S_{11}}(P, k) = \frac{N_1}{m_D(\beta_2 + \chi)} \left[ \frac{1}{\beta_1 + \chi} - \frac{\lambda_{S_{11}}}{\beta_3 + \chi} \right], \quad (\text{A4})$$

where  $\beta_3$  is a new parameter and  $N_1$  is a new normalization constant.  $\lambda_{S_{11}}$  is a parameter that can be fixed, once  $\beta_3$  is known by the orthogonality condition

$$\mathcal{I}_{S_{11}}(0) = 0. \quad (\text{A5})$$

The free parameter  $\beta_3$  can be determined by the fit to the high  $Q^2$  data from the  $\gamma^*N \rightarrow S_{11}(1535)$  transition.

The normalization conditions are

$$\int_k |\psi_N(\bar{P}, k)|^2 = 1, \quad \int_k |\psi_{S_{11}}(\bar{P}, k)|^2 = 1, \quad (\text{A6})$$

where  $\bar{P}$  represents in each case the baryon momentum at the baryon rest frame.

## 2. Fit to the data

In order to extend the application of the model for the  $S_{11}(1535)$  state, also to the low  $Q^2$  regime, we fit Eq. (A1) to the form factor data. The only adjustable parameter available is the value of  $\beta_3$  in the  $\psi_{S_{11}}$  radial wave function, included in the integral  $\mathcal{I}_{S_{11}}$ . As we are taking into account only the valence quark degrees of freedom, we cannot expect a good agreement for small  $Q^2$ , therefore we fit only the high  $Q^2$  data. We consider therefore only the data with  $Q^2 > 1.5 \text{ GeV}^2$ .

Our database includes the data from CLAS [44] ( $Q^2 = 0.3\text{--}4.2 \text{ GeV}^2$ ) and from JLab/Hall C [45] ( $Q^2 = 5.4, 7.0 \text{ GeV}^2$ ). The data from Hall C [45], include only the amplitude  $A_{1/2}$ , assumes that  $S_{1/2}$  is very small, and has very small errorbars. In the fit we double the errorbars from Hall C in order to avoid a high weight from the Hall C data.

The best fit is obtained for  $\beta_3 = 0.540$ . The results for the form factor  $F_1^*$  are presented in Fig. 6, compared with the data mentioned previously, and the data from the MAID analysis [51, 52]. In the same figure we show also the results from the valence quark contributions for the Pauli form factor  $F_2^*$ . We recall that in that case the experimental data (not shown in the graph) is consistent with zero for  $Q^2 > 1.5 \text{ GeV}^2$ . Although one cannot compare directly our model for  $F_2^*$  with the data due to the lack of meson cloud effects we can compare it with other estimates of the quark core effects. In the graph for  $F_2^*$  we present therefore the estimate of the bare core effects given by the EBAC/JLab model [43]. The EBAC model is a coupled-channel reaction model that takes into account the meson and photon coupling with the baryon cores. The result presented in the graph is obtained when the meson cloud effects are removed. As we can see in the graph our results for  $F_2^*$  are very close to the EBAC estimates. That result is remarkable, since no fit relative to the function  $F_2^*$  was considered.

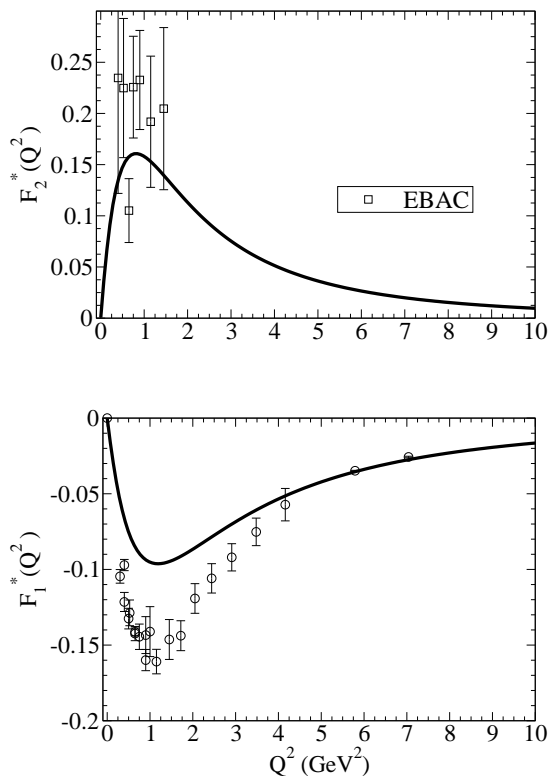


FIG. 6:  $\gamma^*N \rightarrow N^*(1535)$  form factors. Data from CLAS [44] and JLab/Hall C [45]. The EBAC calculations are from Ref. [43].

- 
- [1] I. G. Aznauryan and V. D. Burkert, Prog. Part. Nucl. Phys. **67**, 1 (2012) [arXiv:1109.1720 [hep-ph]].  
 [2] I. G. Aznauryan, A. Bashir, V. Braun, S. J. Brod-

sky, V. D. Burkert, L. Chang, C. Chen and B. El-Bennich *et al.*, Int. J. Mod. Phys. E **22**, 1330015 (2013) [arXiv:1212.4891 [nucl-th]].

- [3] S. Capstick and W. Roberts, *Prog. Part. Nucl. Phys.* **45**, S241 (2000) [nucl-th/0008028].
- [4] R. Koniuk and N. Isgur, *Phys. Rev. D* **21**, 1868 (1980) [Erratum-ibid. *D* **23**, 818 (1981)].
- [5] A. J. G. Hey and J. Weyers, *Phys. Lett. B* **48**, 69 (1974).
- [6] W. N. Cottingham and I. H. Dunbar, *Z. Phys. C* **2**, 41 (1979).
- [7] V. D. Burkert, R. De Vita, M. Battaglieri, M. Ripani and V. Mokeev, *Phys. Rev. C* **67**, 035204 (2003) [hep-ph/0212108].
- [8] V. D. Burkert and T. S. H. Lee, *Int. J. Mod. Phys. E* **13**, 1035 (2004) [nucl-ex/0407020].
- [9] L. Tiator, D. Drechsel, S. Kamalov, M. M. Giannini, E. Santopinto and A. Vassallo, *Eur. Phys. J. A* **19**, 55 (2004) [nucl-th/0310041].
- [10] D. Y. Chen, Y. B. Dong, M. M. Giannini and E. Santopinto, *Nucl. Phys. A* **782**, 62 (2007) [nucl-th/0611016].
- [11] S. Capstick, A. Svarc, L. Tiator, J. Gegelia, M. M. Giannini, E. Santopinto, C. Hanhart and S. Scherer *et al.*, *Eur. Phys. J. A* **35**, 253 (2008) [arXiv:0711.1982 [hep-ph]].
- [12] Y. Dong, M. Giannini, E. Santopinto and A. Vassallo, *Few Body Syst.* **55**, 873 (2014).
- [13] G. Ramalho and K. Tsushima, *Phys. Rev. D* **84**, 054014 (2011) [arXiv:1107.1791 [hep-ph]]; G. Ramalho, K. Tsushima and A. W. Thomas, *J. Phys. G* **40**, 015102 (2013) [arXiv:1206.2207 [hep-ph]].
- [14] G. Ramalho and K. Tsushima, *Phys. Rev. D* **87**, 093011 (2013) [arXiv:1302.6889 [hep-ph]]; G. Ramalho and K. Tsushima, *Phys. Rev. D* **88**, 053002 (2013) [arXiv:1307.6840 [hep-ph]].
- [15] M. Warns, W. Pfeil and H. Rollnik, *Phys. Rev. D* **42**, 2215 (1990).
- [16] S. Capstick and B. D. Keister, *Phys. Rev. D* **51**, 3598 (1995) [nucl-th/9411016].
- [17] R. Bijker, F. Iachello and A. Leviatan, *Phys. Rev. C* **54**, 1935 (1996) [nucl-th/9510001].
- [18] M. Aiello, M. Ferraris, M. M. Giannini, M. Pizzo and E. Santopinto, *Phys. Lett. B* **387**, 215 (1996); M. Aiello, M. M. Giannini and E. Santopinto, *J. Phys. G* **24**, 753 (1998) [nucl-th/9801013].
- [19] R. Bijker, F. Iachello and E. Santopinto, *J. Phys. A* **31**, 9041 (1998) [nucl-th/9801051].
- [20] E. Santopinto, F. Iachello and M. M. Giannini, *Eur. Phys. J. A* **1**, 307 (1998).
- [21] E. Pace, G. Salme, F. Cardarelli and S. Simula, *Nucl. Phys. A* **666**, 33 (2000) [nucl-th/9909025].
- [22] D. Merten, U. Loring, K. Kretzschmar, B. Metsch and H. R. Petry, *Eur. Phys. J. A* **14**, 477 (2002) [hep-ph/0204024].
- [23] E. Santopinto and M. M. Giannini, *Phys. Rev. C* **86**, 065202 (2012)
- [24] M. Ronniger and B. C. Metsch, *Eur. Phys. J. A* **49**, 8 (2013) [*Eur. Phys. J. A* **49**, 8 (2013)] [arXiv:1207.2640 [hep-ph]].
- [25] B. Golli and S. Sirca, *Eur. Phys. J. A* **49**, 111 (2013) [arXiv:1306.3330 [nucl-th]]; B. Golli and S. Sirca, *Eur. Phys. J. A* **47**, 61 (2011) [arXiv:1101.5527 [nucl-th]].
- [26] I. G. Aznauryan and V. D. Burkert, *Phys. Rev. C* **85**, 055202 (2012) [arXiv:1201.5759 [hep-ph]].
- [27] F. Gross, G. Ramalho and M. T. Peña, *Phys. Rev. C* **77**, 015202 (2008) [nucl-th/0606029].
- [28] G. Ramalho and M. T. Peña, *Phys. Rev. D* **84**, 033007 (2011) [arXiv:1105.2223 [hep-ph]].
- [29] G. Ramalho and M. T. Peña, *Phys. Rev. D* **89**, 094016 (2014) [arXiv:1309.0730 [hep-ph]].
- [30] F. Gross, G. Ramalho and M. T. Peña, *Phys. Rev. D* **85**, 093005 (2012). [arXiv:1201.6336 [hep-ph]].
- [31] G. Ramalho, K. Tsushima and F. Gross, *Phys. Rev. D* **80**, 033004 (2009) [arXiv:0907.1060 [hep-ph]].
- [32] G. Ramalho and M. T. Peña, *J. Phys. G* **36**, 115011 (2009) [arXiv:0812.0187 [hep-ph]].
- [33] J. J. Kelly, *Phys. Rev. C* **56**, 2672 (1997).
- [34] Z. Batiz and F. Gross, *Phys. Rev. C* **58**, 2963 (1998) [arXiv:nucl-th/9803053].
- [35] R. A. Gilman and F. Gross, *J. Phys. G* **28**, R37 (2002) [nucl-th/0111015].
- [36] G. Ramalho, M. T. Peña and F. Gross, *Eur. Phys. J. A* **36**, 329 (2008) [arXiv:0803.3034 [hep-ph]].
- [37] G. Ramalho, M. T. Peña and F. Gross, *Phys. Rev. D* **78**, 114017 (2008) [arXiv:0810.4126 [hep-ph]]; G. Ramalho and M. T. Peña, *Phys. Rev. D* **80**, 013008 (2009) [arXiv:0901.4310 [hep-ph]]; G. Ramalho, M. T. Peña and F. Gross, *Phys. Rev. D* **81**, 113011 (2010) [arXiv:1002.4170 [hep-ph]]; G. Ramalho, M. T. Peña and A. Stadler, *Phys. Rev. D* **86**, 093022 (2012) [arXiv:1207.4392 [nucl-th]]; G. Ramalho and M. T. Peña, *Phys. Rev. D* **85**, 113014 (2012) [arXiv:1205.2575 [hep-ph]].
- [38] G. Ramalho and K. Tsushima, *Phys. Rev. D* **81**, 074020 (2010) [arXiv:1002.3386 [hep-ph]]; G. Ramalho and K. Tsushima, *Phys. Rev. D* **82**, 073007 (2010) [arXiv:1008.3822 [hep-ph]].
- [39] G. Ramalho and K. Tsushima, *Phys. Rev. D* **89**, 073010 (2014) [arXiv:1402.3234 [hep-ph]].
- [40] G. Ramalho and K. Tsushima, *Phys. Rev. D* **86**, 114030 (2012) [arXiv:1210.7465 [hep-ph]]; G. Ramalho and M. T. Peña, *Phys. Rev. D* **83**, 054011 (2011) [arXiv:1012.2168 [hep-ph]].
- [41] G. Ramalho, D. Jido and K. Tsushima, *Phys. Rev. D* **85**, 093014 (2012) [arXiv:1202.2299 [hep-ph]].
- [42] G. Ramalho and K. Tsushima, *Phys. Rev. D* **84**, 051301 (2011) [arXiv:1105.2484 [hep-ph]].
- [43] B. Julia-Diaz, H. Kamano, T. S. H. Lee, A. Matsuyama, T. Sato and N. Suzuki, *Phys. Rev. C* **80**, 025207 (2009).
- [44] I. G. Aznauryan *et al.* [CLAS Collaboration], *Phys. Rev. C* **80**, 055203 (2009) [arXiv:0909.2349 [nucl-ex]].
- [45] M. M. Dalton *et al.*, *Phys. Rev. C* **80**, 015205 (2009) [arXiv:0804.3509 [hep-ex]].
- [46] V. I. Mokeev *et al.* [CLAS Collaboration], *Phys. Rev. C* **86**, 035203 (2012) [arXiv:1205.3948 [nucl-ex]].
- [47] J. Beringer *et al.* [Particle Data Group Collaboration], *Phys. Rev. D* **86**, 010001 (2012).
- [48] I. G. Aznauryan, V. D. Burkert, G. V. Fedotov, B. S. Ishkhanov and V. I. Mokeev, *Phys. Rev. C* **72**, 045201 (2005) [hep-ph/0508057].
- [49] M. Dugger *et al.* [CLAS Collaboration], *Phys. Rev. C* **79**, 065206 (2009) [arXiv:0903.1110 [hep-ex]].
- [50] V. I. Mokeev and I. G. Aznauryan, *Int. J. Mod. Phys. Conf. Ser.* **26**, 1460080 (2014) [arXiv:1310.1101 [nucl-ex]].
- [51] D. Drechsel, S. S. Kamalov and L. Tiator, *Eur. Phys. J. A* **34**, 69 (2007) [arXiv:0710.0306 [nucl-th]]; L. Tiator, D. Drechsel, S. S. Kamalov and M. Vanderhaeghen, *Chin. Phys. C* **33**, 1069 (2009) [arXiv:0909.2335 [nucl-th]]; L. Tiator, D. Drechsel, S. S. Kamalov and M. Vanderhaeghen, *Eur. Phys. J. ST* **198**, 141 (2011) [arXiv:1109.6745 [nucl-th]].
- [52] <http://wwwkph.kph.uni-mainz.de/MAID//maid2007/data.html>

- [53] V. Burkert, T. -S. H. Lee, R. Gothe, and V. Mokeev, Electromagnetic N-N\* Transition Form Factors Workshop, Jlab, Newport News, 2008 (unpublished).
- [54] C. E. Carlson and J. L. Poor, Phys. Rev. D **38**, 2758 (1988); C. E. Carlson and N. C. Mukhopadhyay, Phys. Rev. Lett. **81**, 2646 (1998) [hep-ph/9804356].
- [55] V. I. Mokeev, at the 2014 JLab Users Group Meeting, 2014. Jefferson Lab, Newport News, VA, (<http://www.jlab.org/conferences/ugm/program.html>)